Transcriptional Regulation of Arabidopsis Polycomb Repressive Complex 2 Coordinates Cell-Type Proliferation and Differentiation^{OPEN}

Miguel de Lucas,[a,1] Li Pu,[a,2] Gina Turco,[a] Allison Gaudinier,[a] Ana Karina Morao,[b] Hirofumi Harashima,[c] Dahae Kim,[a] Mily Ron,[a] Keiko Sugimoto,[c] Francois Roudier,[b] and Siobhan M. Brady[a,3]

[a] Department of Plant Biology and Genome Center, University of California, Davis, California 95616
[b] Institut de Biologie de l'Ecole Normale Supérieure, Centre National de la Recherche Scientifique, Unité Mixte de Recherche 8197, Institut National de la Santé et de la Recherche Médicale, U1024 Paris, France
[c] RIKEN Center for Sustainable Resource Science, Tsurumi, Yokohama 230-0045, Japan

ORCID IDs: 0000-0002-6544-6404 (M.d.L.); 0000-0002-4350-6760 (A.G.); 0000-0003-3370-4111 (H.H.); 0000-0003-1682-7275 (M.R.); 0000-0002-9209-8230 (K.S.); 0000-0002-1757-6386 (F.R.); 0000-0001-9424-8055 (S.M.B.)

Spatiotemporal regulation of transcription is fine-tuned at multiple levels, including chromatin compaction. Polycomb Repressive Complex 2 (PRC2) catalyzes the trimethylation of Histone 3 at lysine 27 (H3K27me3), which is the hallmark of a repressive chromatin state. Multiple PRC2 complexes have been reported in *Arabidopsis thaliana* to control the expression of genes involved in developmental transitions and maintenance of organ identity. Here, we show that PRC2 member genes display complex spatiotemporal gene expression patterns and function in root meristem and vascular cell proliferation and specification. Furthermore, PRC2 gene expression patterns correspond with vascular and nonvascular tissue-specific H3K27me3-marked genes. This tissue-specific repression via H3K27me3 regulates the balance between cell proliferation and differentiation. Using enhanced yeast one-hybrid analysis, upstream regulators of the PRC2 member genes are identified, and genetic analysis demonstrates that transcriptional regulation of some PRC2 genes plays an important role in determining PRC2 spatiotemporal activity within a developing organ.

INTRODUCTION

The formation of new organs involves transcriptional reprogramming of pluripotent stem cells in order to give rise to different cell types. This temporal and spatial regulation of gene expression is regulated at multiple levels, including chromatin compaction via histone posttranslational modifications, a general mechanism by which promoter accessibility is regulated to enable interaction with transcription factors and RNA polymerase machinery. Despite the extensive chromatin modification data generated in recent years, few studies have evaluated the transcriptional regulation of chromatin modifiers themselves. Polycomb Repressive Complex 2 (PRC2) catalyzes the trimethylation of Histone 3 protein at the lysine 27 position (H3K27me3), the hallmark of a silent chromatin state that is correlated with gene repression and its maintenance across cell division.

PRC2 structure is highly conserved, with four core subunits conventionally named after their homologs in *Drosophila melanogaster*, including an Enhancer of zeste [E(z)] catalytic SET domain-containing protein, an Extra sex combs (Esc) protein, a nucleosome remodeling factor WD40-containing protein (Nurf55), and a Suppressor of zeste 12 zinc finger protein in a stoichiometric ratio of 1:1:1:1 (Ciferri et al., 2012). However, the number of genes that encode each subunit varies between species (Mozgová and Hennig, 2015). The Drosophila genome has been described as containing a single gene for each subunit, which consequently constitute a single complex. However, two copies of the Extra sex combs gene, *ESC* and *ESCL*, have been reported (Ohno et al., 2008). In mouse and human, there are two copies of the E(z) gene, *EZH1* and *EZH2* (Ciferri et al., 2012; Margueron et al., 2008). In addition, distinct isoforms of Esc have been reported in human (Mozgová and Hennig, 2015; Kuzmichev et al., 2005). The *Arabidopsis thaliana* genome encodes three homologous genes for the E(z) methyltransferase subunit, *MEDEA* (*MEA*), *CURLY LEAF* (*CLF*), and *SWINGER* (*SWN*); one for Esc, *FERTILIZATION INDEPENDENT ENDOSPERM* (*FIE*); five WD40-containing protein genes, *MULTICOPY SUPRESSOR OF IRA1-5* (*MSI1-5*); and three Su(z)12, *FERTILIZATION INDEPENDENT SEED2* (*FIS2*), *EMBRYONIC FLOWER2* (*EMF2*), and *VERNALIZATION2* (*VRN2*). Together, these subunits have been reported to form three PRC2 complexes, with the methyltransferases acting partially redundantly (Chanvivattana et al., 2004; Bemer and Grossniklaus, 2012). Several thousand genes are regulated by PRC2, and distinct complexes have been reported to regulate the expression of genes involved in developmental transitions (Zhang

et al., 2007a; Bouyer et al., 2011). The FIS2 complex comprises FIS2, FIE, MEA, and MSI1 and functions in the female gametophyte and endosperm to repress *PHERES* (Köhler et al., 2005). The expression of key regulators of the vegetative-to-reproductive transition, such as *LEAFY* and *AGAMOUS*, are regulated by the EMF2 complex (EMF2, FIE, CLF, or SWN and MSI1) (Kinoshita et al., 2001). A third complex (VRN2), which comprises VRN2, FIE, CLF, or SWN and MSI1, represses *FLOWERING LOCUS C* to accelerate flowering in response to cold (De Lucia et al., 2008).

The regulatory mechanisms that determine which of these complexes are able to act at these specific developmental transitions are unclear. Here, we describe spatiotemporal transcriptional regulation of PRC2 genes in the Arabidopsis root and characterize their function in cellular patterning, proliferation and differentiation. The Arabidopsis root has a simple structural and functional organization consisting of concentric cylinders of cell layers with radial symmetry. Briefly, root growth and development rely on the continuous activity of the apical meristem, where multipotent stem cells surround a small population of centrally located organizing cells, the quiescent center (Scheres, 2007; Terpstra and Heidstra, 2009). Owing to a stereotypical division pattern, stem cells, depending on their position, give rise to different cell files in which the spatial relationship of cells in a file reflects their age and differentiation status (Benfey and Scheres, 2000; Dolan et al., 1993). The epidermis is present on the outside and surrounds the cortex, endodermis, and pericycle layers. The internal vascular cylinder consists of xylem, phloem, and procambium tissues.

Here, we demonstrate that PRC2 controls root meristem development and regulates vascular cell proliferation in the maturation zone. Distinct suites of genes are marked by H3K27me3 in vascular and nonvascular cells to regulate the balance between cellular proliferation and differentiation. Dozens of transcription factors bind to the promoters of genes that encode PRC2 subunits and regulate their expression in Arabidopsis. Together, this multilayered regulatory network provides key insights into the varied means by which gene expression is regulated to ensure appropriate morphogenesis and functioning of a plant organ.

RESULTS

PRC2 Subunits Show Regulated Transcript and Protein Abundance in the Arabidopsis Root

A variety of PRC2 complexes act at distinct developmental transitions during the Arabidopsis life cycle (Kinoshita et al., 2001; Chanvivattana et al., 2004). Spatial and temporal gene expression data in the Arabidopsis root (Supplemental Figure 1) suggest that transcriptional regulation may be an important component in determining the presence of specific PRC2 genes in different cell types. SWN, EMF2, and VRN2 proteins have previously been reported in the root meristem and in root hairs (Ikeuchi et al., 2015). To further validate the spatiotemporal expression pattern of PRC2 subunits, we generated transcriptional fusions for each PRC2 gene (Figures 1A to 1H) and studied the respective reporter expression pattern within the root. *MEA* was not expressed within the root, while *FIS2* was expressed in the columella (Figures 1C and 1F). The potential promoter regions of most subunits drove strong

expression in all cell types in the meristematic zone that then became preferentially detectable in the vascular cylinder in the elongation and maturation zones (Figures 1A to 1H). *CLF* in particular showed enrichment in the root vasculature in both the meristem and maturation region of the root, and this was corroborated by an in situ hybridization with a probe to the *CLF* transcript (Figure 1E; Supplemental Figure 2D). Translational fusions, for all but FIS2, were then used to determine if further regulatory mechanisms might also affect PRC2 protein abundance. SWN protein abundance was enriched within the epidermal and ground tissue layers in the meristem (Figure 2C). The CLF protein, in a complemented *clf-29* mutant background, was found in the root meristem and enriched in the vascular tissue in the maturation zone (Figure 2E; Supplemental Figure 3B). CLF protein in a complemented *clf-28 swn-7* background shows the same enrichment patterns (Supplemental Figure 2E). Within the root meristem and elongation zone, SWN, EMF2, VRN2, and FIE (in a complemented *fie-1* mutant background) proteins are present (Figures 2A to 2C and 2F). In the differentiation zone, however, SWN, EMF2, VRN2, and FIE proteins are present primarily in vasculature (Figures 2A, 2B, 2C, and 2F), although VRN2, EMF2, and SWN proteins have also been reported in root hairs (Ikeuchi et al., 2015).

PRC2 Activity Is Required for Proper Root Development

The expression and protein abundance patterns of PRC2 genes suggested that PRC2 might influence cell patterning or specification in the Arabidopsis root. Since the MEA protein is not found within the Arabidopsis root, CLF and SWN are the only methyltransferases that are candidate regulators of root development. To test the consequences of loss of PRC2 in root cell specification and patterning, we analyzed the phenotypes of *clf-28 swn-7* mutants, which produce viable embryos with PRC2 function eliminated after germination. In agreement with Lafos et al. (2011), the *clf-28 swn-7* mutants showed a complete loss of H3K27me3 deposition, as revealed using whole-mount immunocytochemistry (Figures 3A and 3B). However, both the *clf-29* and *swn-7* single mutants show nuclear H3K27me3 (Supplemental Figures 3 and 4), suggesting that these proteins have partially redundant functions. Analysis of the single and double mutant combinations of CLF and SWN demonstrated that they interact genetically. The *swn-7* allele has a shorter root with no difference in meristem size, while *clf-29* shows no difference in root length but has a significant increase in the number of cells in the root meristem, as previously reported (Figures 3J and 3K) (Aichinger et al., 2011). The roots of *clf-28 swn-7* double mutants are shorter than those of the wild type, with a small meristem containing fewer cells (Figures 3C, 3D, 3J, and 3K), as does the *clf-29 swn-7* double mutant (Supplemental Figures 5C and 5D). Although no defects in radial cell patterning were observed, the number of cells in the vascular cylinder was significantly increased (Figures 3E to 3G and 3I; Supplemental Figure 5A). In striking similarity with the *clf-28 swn-7* phenotype, the *fie* mutant (Bouyer et al., 2011) displayed a smaller meristem with fewer cells (Supplemental Figure 5B) in addition to a large increase in the number of cells within the vascular cylinder (Figure 3G). This increase in vascular cell number was characterized by an increase in protoxylem and metaxylem cells (Figures 3L and 3M).
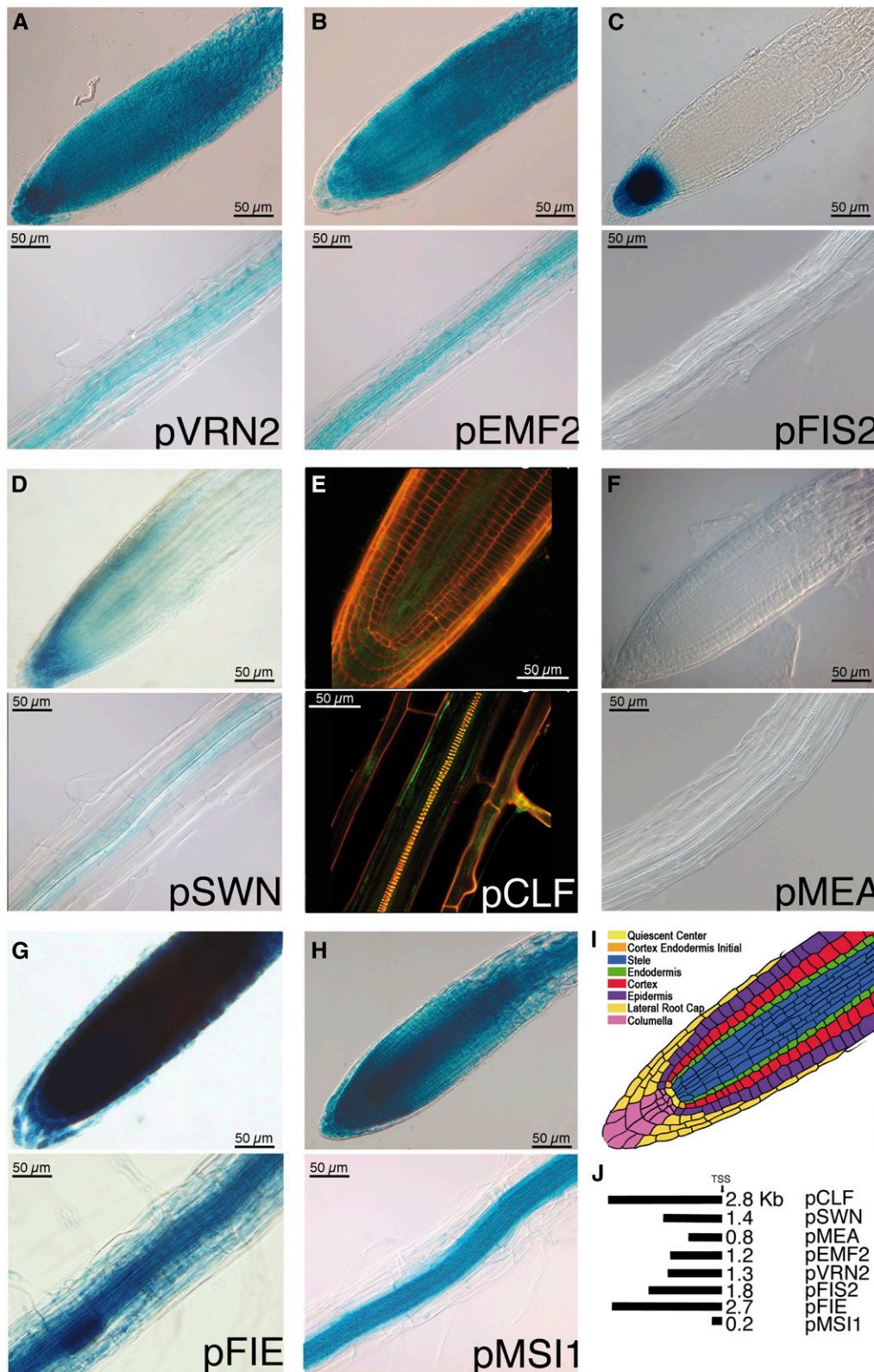
Figure 1. PRC2 Genes Are Expressed in Unique and Overlapping Cell Types in the Arabidopsis Root.

For each genotype, the top panel shows the root meristem, while the bottom panel shows the maturation/differentiation zone of the root. All images were taken under the same acquisition conditions.

(A) VRN2$_{pro}$:GUS expression.

(B) EMF2$_{pro}$:GUS expression.

Although there are several MSI1 homologs, immunopurification experiments determined that MSI1 is the primary WD40 protein required for PRC2 activity in Arabidopsis (Derkacheva et al., 2013). It should be noted, however, that MSI1 is also a member of other chromatin modifying complexes (Jullien et al., 2008). Given the vascular phenotypes of mutations in other PRC2 genes and in order to circumvent the female gametophytic lethality of *msi1* mutants (Köhler et al., 2003), we generated a transgenic line that expressed an artificial miRNA (amiRNA) targeting *MSI1* under the *WOODEN LEG* (*WOL*) promoter (WOL$_{pro}$:amiRNA_MSI1) (Inoue et al., 2001), the expression of which is restricted to the vascular cylinder of the root. To validate *MSI1* silencing, we introduced the transgene into a line containing MSI1$_{pro}$:MSI1:GFP (Figures 3N and 3O). We tested for changes in H3K27me3 deposition in MSI1 silenced lines and observed a reduction specifically in the vascular cylinder (Supplemental Figure 6). The MSI1$_{pro}$:MSI1:GFP signal was undetectable in the WOL$_{pro}$:amiRNA_MSI1 vascular cylinder (Figures 3I and 3J). Silencing of *MSI1* in the vascular cylinder was sufficient to decrease overall root growth (Figures 3P and 3Q), with fewer cells in the meristem, similar to the phenotypes observed in *clf-28 swn-7* and *fie*. However, in contrast with *clf-28 swn-7* and *fie*, which showed an increase in cell number, a statistically significant decrease in vascular cell number was observed (Figures 3G and 3M). Taken together, our results indicate that PRC2 regulates both root meristem cell number and vascular cell proliferation.

Genes Specifically Marked by H3K27me3 in Vascular and Nonvascular Tissue

Many genes marked by H3K27me3 have distinct cell type or tissue-specific expression patterns (Turck et al., 2007; Zhang et al., 2007a; Deal and Henikoff, 2010; Lafos et al., 2011), and the data presented above suggested that PRC2 likely regulates the expression of many genes in the vasculature as well as in other cell types within the root. In order to identify the genes specifically marked by H3K27me3 in the vascular tissue relative to the whole root, we performed fluorescence-activated cell sorting using the WOL$_{pro}$:GFP marker line (Birnbaum et al., 2003) (Supplemental Figures 7A to 7C) coupled with chromatin immunoprecipitation (ChIP)-seq using an antibody specific for H3K27me3. As a control, we also performed ChIP-seq with an antibody specific for H3K4me3, a chromatin modification associated with expressed genes. As expected from previous reports (Zhang et al., 2007b; Roudier et al., 2011), genes marked with H3K27me3 showed lower expression relative to genes with H3K4me3 (Figure 4A).

Comparison between the list of genes marked by H3K27me3 in the WOL$_{pro}$ population and in the root protoplast population (Figure 4B) identified 130 genomic regions marked by H3K27me3 specifically in the vascular cylinder (Figure 4B). In comparison, 2859 genes were specifically enriched in H3K27me3 outside of the vascular tissue (Supplemental Data Set 1). To identify biological processes overrepresented in H3K27me3-marked regions associated with the WOL$_{pro}$:GFP sorted population relative to the whole root population, we performed Gene Ontology (GO) enrichment analysis (Du et al., 2010). Among these lists of H3K27me3-marked genes, 113 and 82 GO categories were significantly enriched in the WOL$_{pro}$:GFP population and the whole root population, respectively (Supplemental Data Set 1). Thirty-seven GO terms were enriched only in the WOL$_{pro}$:GFP population, while six GO terms were enriched only in the whole root population and thus may represent non-vascular-specific GO terms, although they were not significantly underrepresented within the WOL$_{pro}$:GFP population (Supplemental Figure 6D and Supplemental Data Set 1). The set of non-vascular-specific GO terms are consistent with repression of biological processes associated with vascular development and include axis specification, adaxial/abaxial pattern formation, meristem maintenance, phloem or xylem histogenesis, xylem development, and cell wall organization or biogenesis. In the WOL$_{pro}$:GFP-specific samples, H3K27me3-marked genes were enriched for floral development, gibberellin-related processes, and terpenoid metabolism, suggesting differential regulation of these pathways within vascular cells.

Functional Importance of Tissue-Specific PRC2-Mediated Repression

In order to identify H3K27me3-marked genes that are transcriptionally repressed in the vascular cylinder or in nonvascular cells, we further restricted the lists of H3K27me3-marked genes using cell-type-specific gene expression data (Brady et al., 2007). The auxin response factor *ARF17* is marked specifically by H3K27me3 in vascular tissue and is not expressed in the vascular cylinder. This nonvascular expression pattern was confirmed using a transcriptional fusion in which GFP is expressed under the *ARF17* promoter (Figure 4C) (Okushima et al., 2005). Conversely, *VND7*, a well-described regulator of vascular development, was marked by H3K27me3 in nonvascular cells and is specifically expressed in vascular tissue, as confirmed by the use of a promoter:reporter (YFP) fusion (Yamaguchi et al., 2010) (Figures 4E and 4F).

Figure 1. (continued).

(C) FIS2$_{pro}$:GUS expression.
(D) SWN$_{pro}$:GUS expression.
(E) CLF$_{pro}$:VenusN7 expression.
(F) MEA$_{pro}$:GUS expression.
(G) FIE$_{pro}$:GUS expression.
(H) MSI1$_{pro}$:GUS expression.
(I) Cartoon of the different cell types and tissues in the Arabidopsis root.
(J) Promoter lengths of the different PRC2 genes used in the reporter lines. TSS, translational start site.
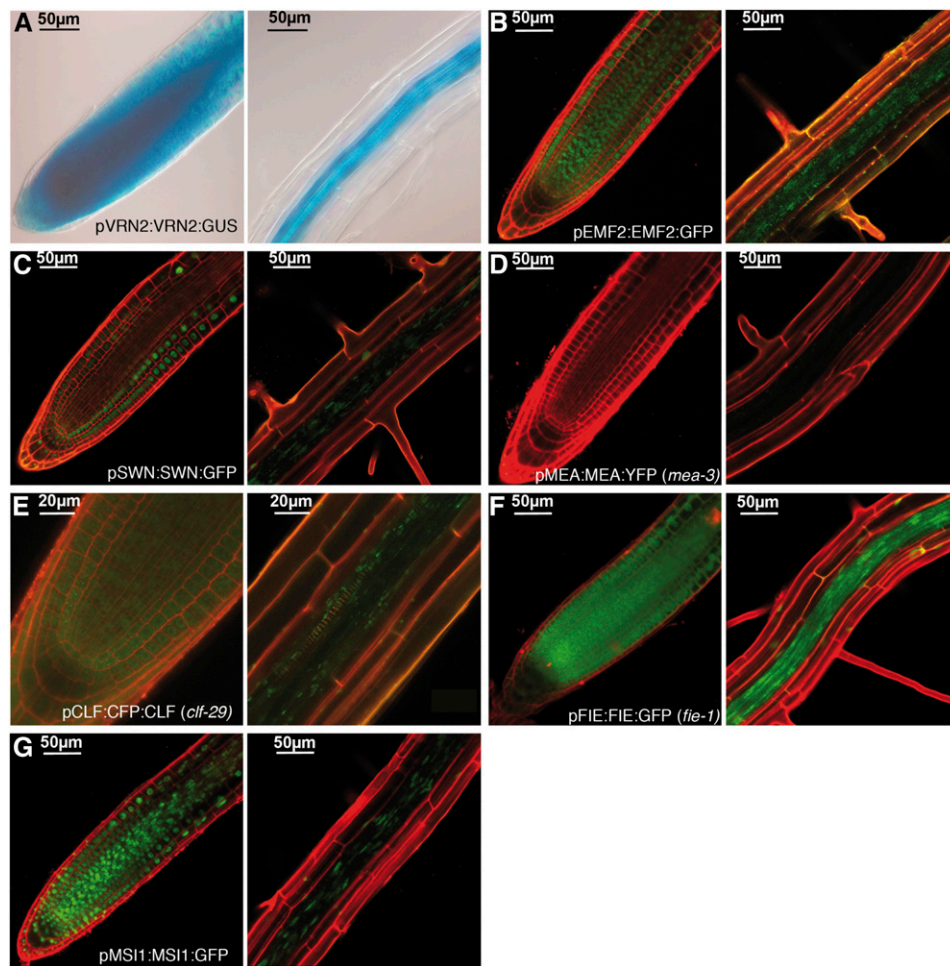
Figure 2. PRC2 Proteins Are Found in Unique and Overlapping Cell Types in the Arabidopsis Root.

For each genotype, the left panel shows the root meristem, while the right panel shows the maturation/differentiation zone of the root.
(A) VRN2$_{pro}$:VRN2:GUS.
(B) EMF2$_{pro}$:EMF2:GFP.
(C) SWN$_{pro}$:SWN:GFP.
(D) MEA$_{pro}$:MEA:YFP in *mea-3.*
(E) CLF$_{pro}$:CFP:gCLF in *clf-29*.
(F) MSI1$_{pro}$:MSI1:GFP.
(G) FIE$_{pro}$:FIE:GFP in *fie-1*.

In order to determine the functional importance of PRC2-mediated repression, we sought to override/bypass the silencing in the vasculature presumably conferred by the PRC2 by expressing *ARF17* under the control of a β-estradiol-inducible promoter (Coego et al., 2014). This is a similar approach to one described for AGAMOUS, a PRC2 target gene (Sieburth and Meyerowitz, 1997), and other target genes (Ikeuchi et al., 2015). The constitutive induction of *ARF17* in the root caused a loss of organization of the root pattern, with frequent observations of ectopic cell proliferation (Figures 4G to 4J; Supplemental Figure 3A). In contrast, ectopic expression of VND7 with the β-estradiol-inducible promoter induced ectopic xylem cell differentiation, as has been previously reported (Kubo et al., 2005) (Figures 4E, 4F, 4K, and 4L). Thus,

these PRC2-target genes regulate the correct balance between cell proliferation and cell differentiation.

Transcriptional Regulation of PRC2 Core Components in the Arabidopsis Root

The differential spatiotemporal expression patterns of PRC2 genes suggest a regulatory role for transcription factors in determining this specificity. We thus utilized the 5′ flanking regions upstream of the translational start site of PRC2 genes in the synthesis of the transcriptional fusions as bait in an enhanced yeast one-hybrid assay (Brady et al., 2011; Taylor-Teeples et al., 2015). In order to focus on the vascular-specific regulation of these genes, we screened the promoters against a set of root
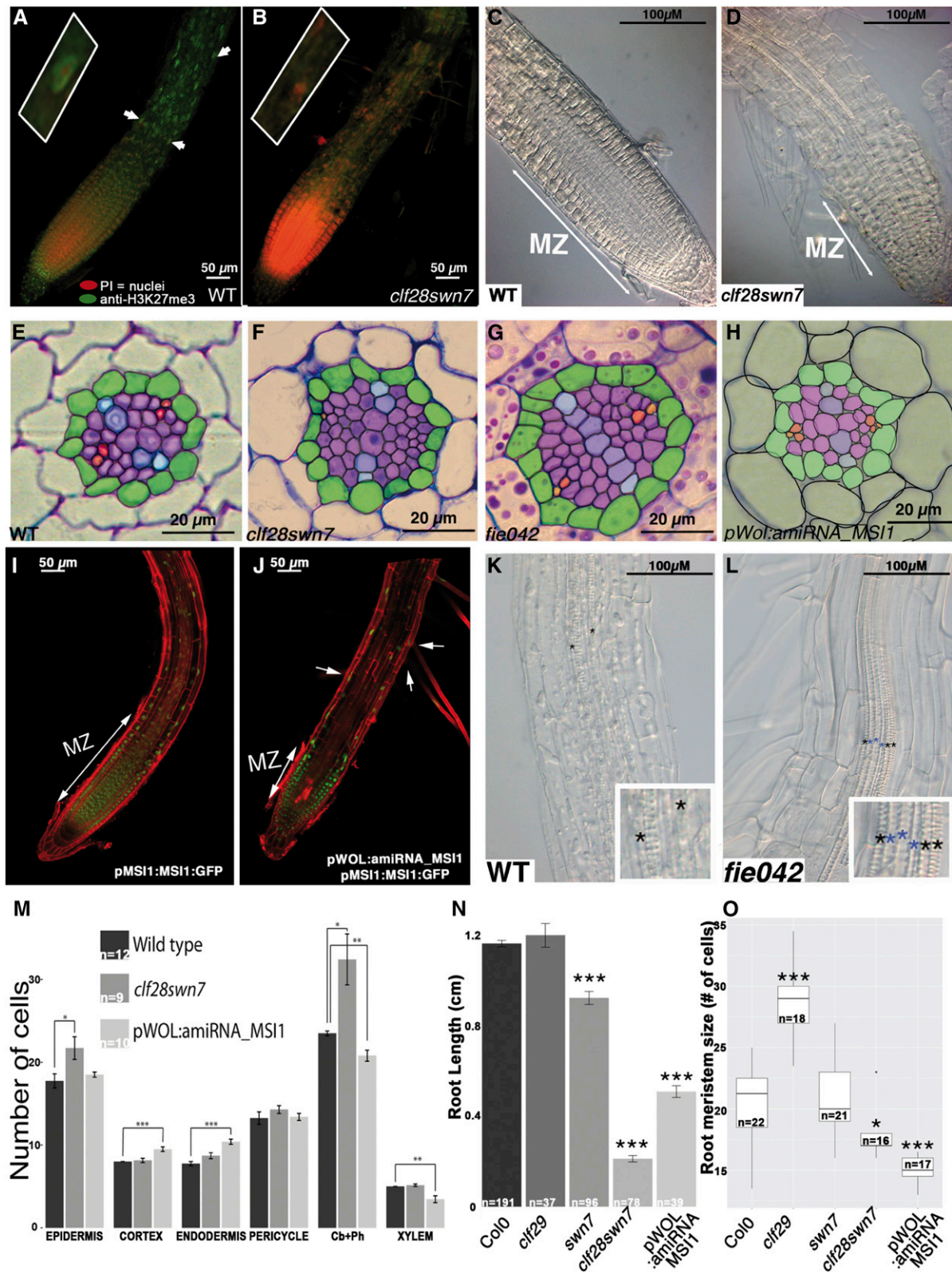
Figure 3. PRC2 Regulates Cell Proliferation in the Root Meristem and Vascular Cylinder.

(A) and **(B)** Whole-mount immunostaining with antibodies specific for H3K27me3 (green in the wild-type Col-0) **(A)** and in the *clf-28 swn-7* double mutant **(B)**. Nuclear staining is indicated with white arrows. A magnified nucleus is shown in the inset.

(C) and **(D)** Differential interference contrast image of the root meristem of the wild-type Col-0 **(C)** and the *clf-28 swn-7* double mutant **(D)**. White lines indicate the root meristematic zone (MZ).

vascular-expressed transcription factors (Gaudinier et al., 2011) (Supplemental Data Set 2). In total, 101 transcription factors (TFs; out of 653) interacted with these potential promoters (Figure 5), with 10 TF families overrepresented (C2H2, bHLH, Homeobox, MYB, AP2-EREBP, WRKY, GRAS, bZIP, C2C2-Dof, and ARF; P value < 0.01). In order to validate these transcription factor-promoter interactions in planta, we performed two types of assays. Transcription factors were overexpressed using a β-estradiol-inducible system (Coego et al., 2014) and expression of the respective target gene was measured 24 h after induction (Supplemental Data Set 3). In addition, myc-tagged transcription factors were assessed for their ability to drive expression of the GUS reporter gene fused to the target promoter in *Nicotiana benthamiana* leaves (Supplemental Data Set 3). Altogether, 71 of the 101 transcription factors in the network were tested in these in planta assays and a total of 63 interactions were successfully validated in planta (Figure 5; Supplemental Data Set 3 and Supplemental Figure 8). We hypothesize that these transcription factors represent an important upstream regulatory component of PRC2 gene expression. We next postulated that distinct TFs could control the expression of PRC2 genes in different cell types. To address this question, we investigated the coexpression patterns between each TF and their target gene using spatial root transcriptome data (Brady et al., 2007) (Supplemental Figure 7). A total of nine TF-promoter interactions were significantly and highly correlated across cell types ($r \geq \pm 0.6$) (Supplemental Data Set 3). Together, our data demonstrate that a diverse set of transcription factors is sufficient to regulate PRC2 expression in planta, along with other factors including the regulation of the chromatin environment, which likely act in a combinatorial regulatory code to specify PRC2 gene expression.

Transcriptional Regulation of PRC2 Components Contributes to PRC2-Mediated Regulation of Cell Proliferation and Differentiation

In order to determine the functional contribution of transcription factors controlling PRC2 gene expression that in turn regulate the expression of PRC2 target genes, we focused on the DOF6 transcription factor, which activates *CLF* expression both in transient and estradiol induction assays (Supplemental Data Sets 1 and 3). The induction of *DOF6* causes severe inhibition of root growth but increases the number of cells in the meristem (Figure 6A; Supplemental Figures 2A and 2B). Both *DOF6* and *CLF* are also expressed in root vascular tissue, further supporting the possibility of this regulatory interaction in planta (Rueda-Romero et al., 2012) (Figure 1E; Supplemental Figures 2C and 2D). Since DOF6 is sufficient to increase *CLF* expression (Figure 6C), our hypothesis was that DOF6 overexpression could lead to an increase in *CLF* expression in nonvascular tissue, which in turn could result in an increase in PRC2 activity in these cell types, as determined by measuring gene expression and corresponding H3K27me3 levels. Our H3K27me3 ChIP-seq data demonstrate that *ARF17* is a vascular-specific target of PRC2, and the transcriptional fusion data demonstrate that *ARF17* is only expressed outside of the vasculature (Figure 4C; Supplemental Data Set 1). *ARF17* is a target of PRC2 complexes containing CLF but not SWN based on the increase in gene expression in *clf-29* versus *swn-7* mutants (Figure 6B). Furthermore, overexpression of a miRNA160-resistant version of ARF17 results in prominent vegetative and floral defects similar to those observed in *clf-29*, including upward curling of leaf margins, reduced plant size, accelerated flowering time, and reduced fertility (Mallory et al., 2005). We thus chose ARF17 as a candidate to explore the influence of PRC2 gene expression manipulation on its target gene (*ARF17*) expression.

Overexpression of *DOF6* led to increased expression of *CLF* concomitantly with a decrease in *ARF17* expression (Figure 6C). This decrease in *ARF17* expression is dependent on CLF, as shown in the DOF6 estradiol-inducible line in the *clf-29* mutant background (Figure 6E). Furthermore, the domain of *ARF17* expression expanded to the vascular cylinder in a *clf-29* mutant background (Figure 6F), demonstrating that CLF is sufficient to regulate the spatial expression pattern of *ARF17*. Finally, H3K27me3 of *ARF17* is increased upon *DOF6* induction (Figure 6D), demonstrating that *DOF6* increases the expression of *CLF* and, in turn, CLF regulates the expression of the target gene *ARF17* through changes in H3K27me3. An additional influence of CLF was observed with respect to the regulation of root length. When the *clf-29* mutation was introduced into the DOF6 estradiol-inducible line, upon estradiol induction, no influence on root length was observed. Thus, we identified transcription factors that are sufficient to control the expression of PRC2 genes in the root, and we demonstrated that altered expression of these transcription factors can disrupt the expression of a PRC2 subunit gene in addition to the levels of H3K27me3 and the corresponding expression of its target gene.

Figure 3. (continued).

(E) to **(H)** Cross sections showing the root vascular cylinder in wild-type Col-0 **(E)**, *clf-28 swn-7* **(F)**, *fie042* **(G)**, and the WOL_pro:amiRNA_MSI line **(H)**. Green indicates pericycle cells, purple indicates procambium cells, and red/orange indicates phloem cells.

(I) and **(J)** The MSI protein is expressed ubiquitously throughout the Arabidopsis root **(I)** but is depleted specifically from the vascular cylinder in the WOL_pro:amiRNA_MSI1 line in the MSI1_pro:MSI1:GFP background (white arrows with one head) **(J)**. Note the reduction in the length of the root meristem (white arrow with two heads).

(K) and **(L)** Differential interference contrast image showing two protoxylem pole cell files (black asterisk) in the wild-type Col-0 **(L)** and ectopic protoxylem (black asterisk) and metaxylem (blue asterisk) in the *fie042* mutant background **(L)**.

(M) There are significantly more procambium and phloem and epidermal cells in the *clf-28 swn-7* mutant compared with wild-type Col-0. The reduction in *MSI1* expression shows increased number of cortical and endodermal cells but lower levels of cells in the stele.

(N) The roots of *swn-7*, *clf-28 swn-7*, and WOL_pro:amiRNA_MSI are significantly shorter than wild-type Col-0 and *clf-29*.

(O) There are more cells in the meristem of *clf-29* and fewer in *clf-28 swn-7* and WOL_pro:amiRNA_MSI relative to the wild type (Col-0). In all cases, significance was tested using a *t* test. *P < 0.05, **P < 0.01, and ***P < 0.001. Error bars indicate SE.
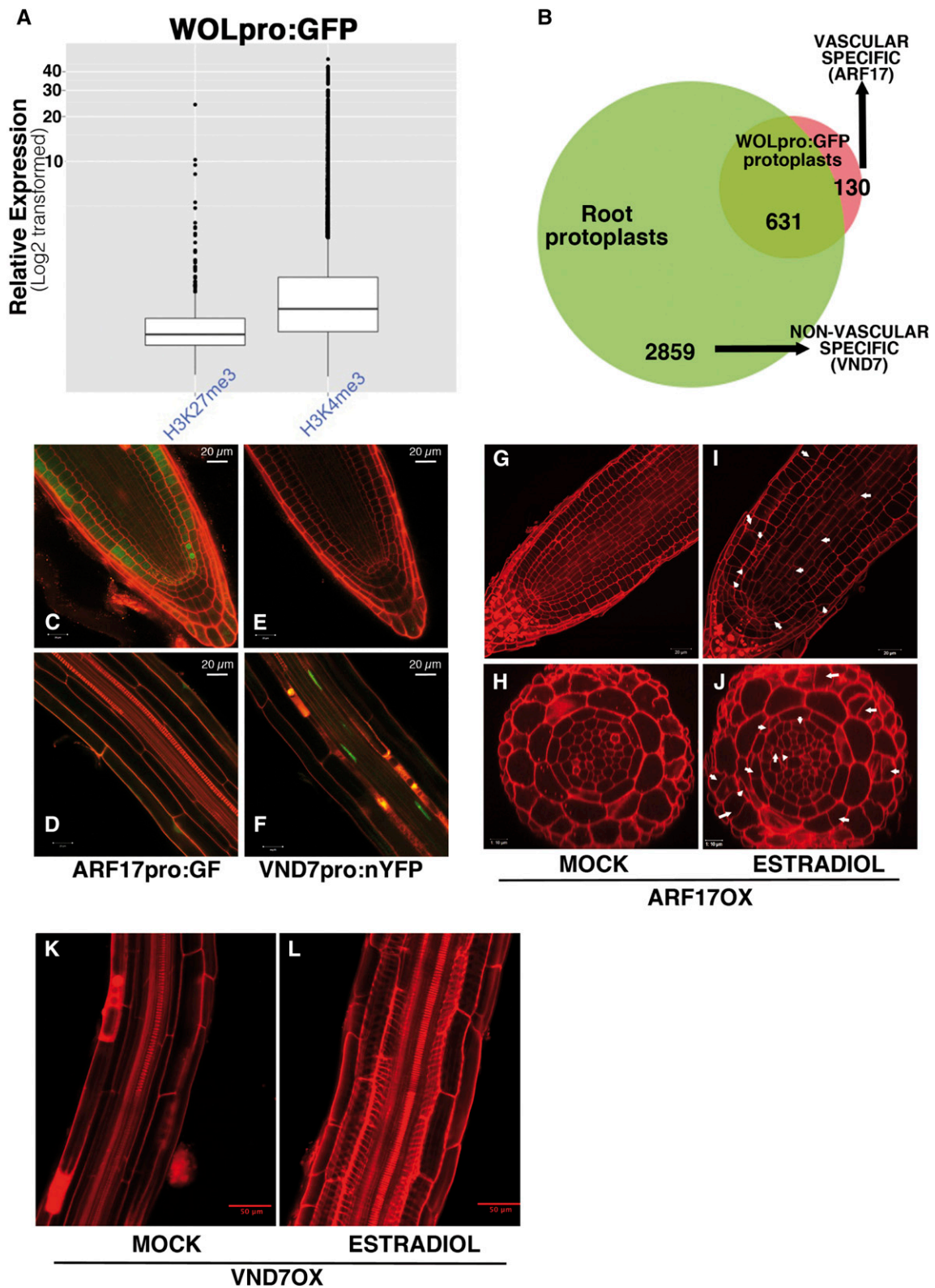
Figure 4. PRC2 Regulates the Balance between Cell Proliferation and Differentiation in a Tissue-Specific Manner in the Arabidopsis Root.

(A) Expression levels of genes marked by H3K27me3 in vascular cells relative to expression levels of genes marked by H3K4me3. Whole-root and vascular-specific (pWOL:GFP positive) root protoplast were isolated by fluorescence-activated cell sorting and H3K27me3/H3K4me3-enriched regions were resolved by ChIP-seq. Expression of the vascular specific H3K27me3 and H3K4me3 marked genes was determined using Brady et al. (2007) transcriptional data.
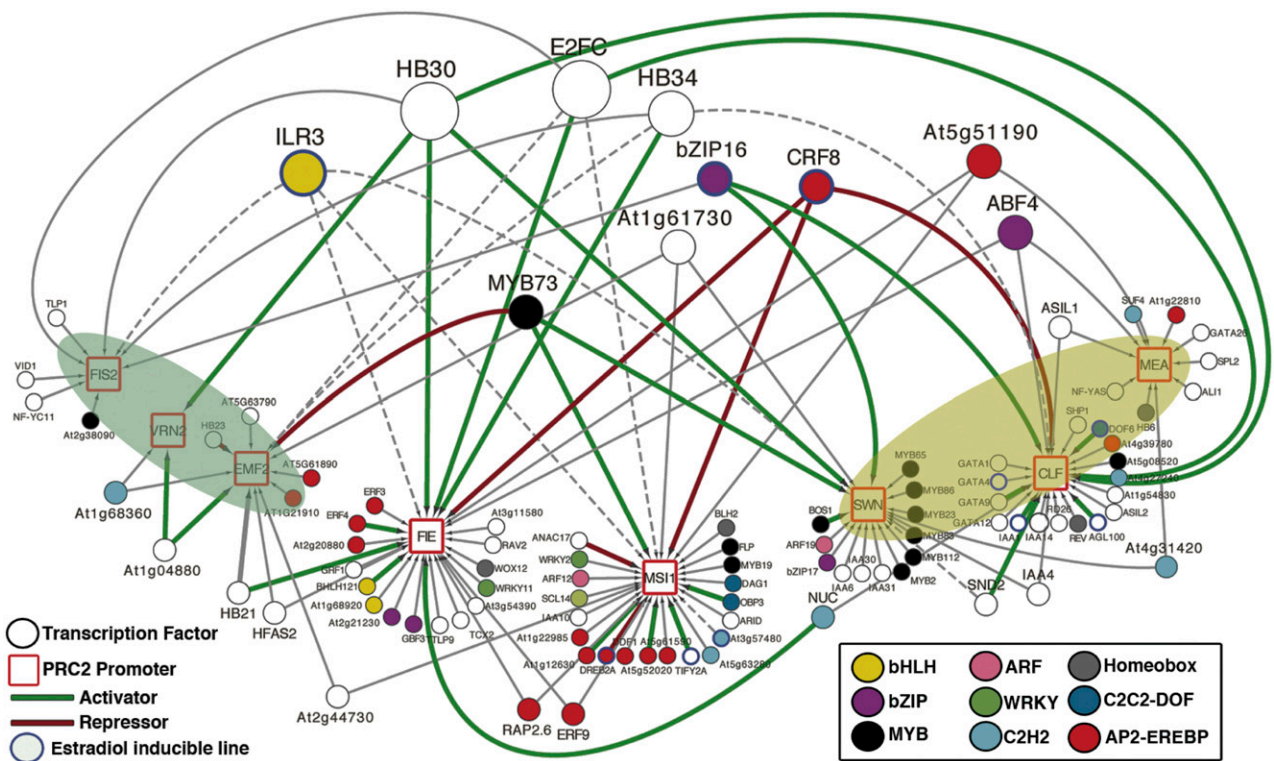**(B)** Number of genes marked by H3K27me3 in nonvascular cells.

Figure 5. Transcription Factors Regulating PRC2 Gene Expression in Planta.

Squares represent PRC2 gene promoters, and circles represent transcription factors. A line between a transcription factor and promoter indicates that an interaction was observed by yeast one-hybrid analysis. A green line or a red line indicates that the transcription factor has been validated in planta as activating or repressing, respectively, the target gene in planta in either a transactivation assay or upon β-estradiol induction of the transcription factor. Transcription factors are additionally colored according to their respective family. Transcription factors that interact with the most PRC2 gene promoters are indicated at the top of the network, while transcription factors that interact with just a single promoter are located just beside their respective PRC2 gene promoter. Network information is available in Supplemental Data Set 1.

DISCUSSION

A Multitiered Regulatory Network for Gene Expression

We systematically characterized the regulation of PRC2 gene expression at cell-type resolution using Arabidopsis roots as a model system. We showed that there are distinct spatial and temporal transcript accumulation patterns for PRC2 components. The heterologous (yeast/*N. benthamiana*) and in vivo (Arabidopsis) approaches we employed revealed a transcriptional network that controls PRC2 gene expression in the Arabidopsis root. Altogether, our data provide evidence that transcriptional control of the PRC2 component *CLF*, and likely of other PRC2

components, plays an important role in determining H3K27me3 levels and the corresponding expression of H3K27me3 targets in a spatiotemporal manner. This regulation is likely complemented by other previously described modes of regulation in Arabidopsis, including *cis*-regulatory regions similar to the Polycomb repressive element in Drosophila (Deng et al., 2013), long noncoding RNAs, and protein-protein interactions via PRC1 and PRC1-like genes to determine target specificity and chromatin compaction (Margueron and Reinberg, 2011).

Further dissection of these distinct tiers of this regulatory network is needed. At the upper level of the network, the correlation of expression between transcription factors and their target PRC2 genes (Brady et al., 2007) suggests that distinct groups of

---

Figure 4. (continued).

(C) and **(D)** Expression of a gene marked specifically by H3K27me3 in the vascular cylinder and not expressed in vascular cells: ARF17pro:GFP.
(E) and **(F)** Expression of a gene marked by H3K27me3 in the root, but not in the vascular cylinder, and not expressed in nonvascular cells: VND7pro:nYFP.
(G) to **(J)** Estradiol induction of the ARF17 transcription factor results in small regions of additional cell proliferation in the vascular cylinder (**[I]** and **[J]**) compared with the mock-treated root (**[G]** and **[H]**). Asterisks indicate ectopic cell proliferation.
(K) and **(L)** Estradiol induction of the VND7 transcription factor **(L)** results in ectopic xylem cell differentiation compared with a mock-treated root **(K)**.
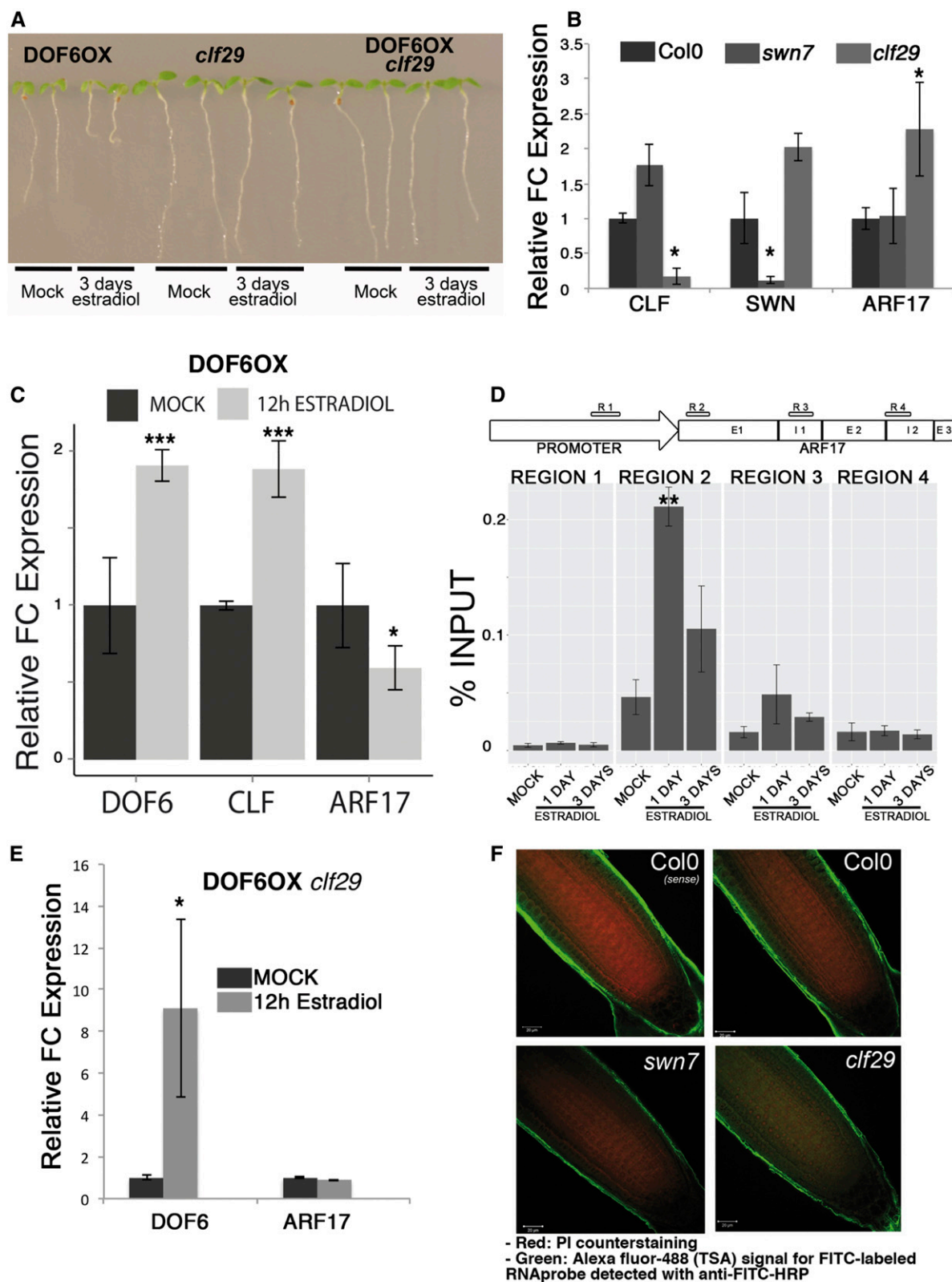
Figure 6. Functional Validation of a Multitier PRC2 Gene Regulatory Network (TF→ PRC2 Gene → H3K27me3-Regulated Gene).

(A) β-Estradiol induction (3 d) of the DOF6 transcription factor results in a significantly shorter root. Root inhibition caused by the induction of *DOF6* is abolished in the *clf29* background.
(B) ARF17 expression is activated in the *clf-29* mutant.

transcription factors regulate the expression of these genes in space, in time, or in both space and time (Supplemental Data Set 1). At the second tier of the network, analyses of PRC2 gene mutants demonstrated that CLF, SWN, and FIE, key components of PRC2, functionally regulate root meristem and vascular development, likely at the level of cell division. Additionally, the translational fusion patterns suggest that only a restricted number of complexes can form at a particular cell type or temporal stage of development. It will be interesting in the future to determine if the cell-type- or tissue-specific expression patterns of *CLF* or *SWN* are necessary to regulate the H3K27me3 of distinct suites of genes. In addition, in proximal meristematic vascular tissue, CLF and SWN protein were both present. The mechanism by which different complexes form and how the affinity for different targets is determined remain to be described. At the final tier of the network, whether distinct PRC2 complexes regulate distinct groups of genes within the root meristem remains to be determined. However, our data showing vascular-specific H3K27me3 and silenced genes provide proof of such suites of genes at the level of individual tissues.

Regulation of Cell Proliferation and Differentiation during Arabidopsis Root Development

In plants, PRC2 proteins maintain organ and cell-type identity, regulate developmental transitions, repress cell proliferation (Lafos et al., 2011; Hennig and Derkacheva, 2009), and regulate totipotency (He et al., 2012). Here, we report two additional functions of PRC2 in postembryonic development: the regulation of cell proliferation in vascular tissue and the appropriate execution of xylem cell differentiation (Figures 3E to 3G, 3L, and 3M). In the developing root, procambium cells are the stem cell source responsible for vascular cell types and secondary growth (Mähönen et al., 2006, 2000; De Rybel et al., 2014). Procambium cells proliferate and can undergo differentiation into either xylem cells or phloem cells depending on positional cues (Fisher and Turner, 2007; Etchells et al., 2013; Etchells and Turner, 2010). The vascular proliferation phenotype of the *clf-28 swn-7* mutant suggests that PRC2 represses division of the procambium cell population. *CLF* and *SWN* are not responsible for initiating division of these cells, but rather, when the appropriate number of cells has been produced, PRC2 activity likely negatively influences chromatin accessibility for transcription factors such as *ARF17* in addition to cell cycle regulators. The overproliferation phenotype of the *ARF17* overexpressor and its similarity to the phenotype of the *clf28swn7* mutant suggest that ARF17 may be such a cell cycle regulator. The lack of a vascular

phenotype in the *clf29* mutant implies that cell proliferation is likely also controlled by other SWN-dependent H3K27me3 targets. On the other hand, the *fie-042* ectopic xylem cell phenotype, the tissue-specific VND7 H3K27me3 deposition pattern, and the finding that overriding this repression through ectopic expression results in ectopic xylem differentiation suggest that tissue-specific PRC2 activity ensures the appropriate execution of the xylem cell differentiation program.

Knockdown of *MSI1* in the vascular tissue resulted in a very different phenotype relative to that observed in mutants of other PRC2 subunits. In the vascular cylinder, the planes of division were altered, suggesting that this particular gene likely plays a role in procambium cell patterning. Interestingly, WOL$_{pro}$:amiRNA_MSI1 expression resulted in a short root phenotype despite being only driven in the vascular cylinder. This could be due to cell nonautonomous effects, defects in vascular development influencing overall growth, or a defect in the vascular initial cells, which determine quiescent cell identity. MSI1 is a member of other chromatin modifying complexes, including the CAF1 complex, which is associated with nucleosome deposition for chromatin assembly and histone deacetylation (Hennig et al., 2003). Thus, the phenotypes observed may reflect developmental decisions occurring during early root patterning or independent of PRC2 activity.

A Comparative Perspective on PRC2 Function in Plants and Animals

In animal embryonic stem cells and outside of the embryo, PRC2 is required for the maintenance of differentiation potential (Laugesen and Helin, 2014). Mutations in PRC2 subunits can either delay differentiation of myogenic or neurogenic cell types or precociously advance the differentiation of particular cell types in addition to preserving the appropriate cell identity (Stojic et al., 2011; Pasini et al., 2007; Hirabayashi et al., 2009; Fasano et al., 2007; Sher et al., 2008; Aldiri and Vetter, 2009). In contrast, in the plant procambial stem cell population, PRC2 regulates self-renewal capabilities. Our data also demonstrate that in root cells, PRC2 ensures the correct cell-type-specific differentiation state through spatially repressing the expression of cell-type-specific developmental regulators (VND7). Thus, in plants, PRC2 regulates self-renewal of the procambial stem cell population in addition to cell differentiation.

Uncontrolled abundance, increased activity, or loss of function of PRC2 components can lead to disease (Bracken et al., 2003; Kleer et al., 2003; Takawa et al., 2011; Varambally et al., 2002; Wagener et al., 2010). Thus, our findings indicate that transcription

---

Figure 6. (continued).

(C) Induction of DOF6 results in a significant increase in the amount of *CLF* expression and a corresponding repression of *ARF17* expression, as revealed by RT-qPCR.

(D) Induction of DOF6 results in a significant increase in H3K27me3 deposition in the *ARF17* loci in the root tissue.

(E) DOF6 induction does not affect *ARF17* expression in the *clf-29* background.

(F) Whole-mount in situ hybridization of *ARF17* mRNA. *ARF17* expression domain is expanded toward the vascular cylinder in the *clf-29* mutant. In all cases, significance was tested using a *t* test. *P < 0.05, **P < 0.01, and ***P < 0.001. Error bars represent the SE value of the log$_2$-transformed expression. The mean is from three independent experiments (biological replicates), calculated from the average of three technical replicates per biological replicate. Each biological replicate captures expression from ~200 roots of each respective genotype. In each case, the ΔΔCt was calculated relative to a ubiquitin10 control.

factors may be an important component in determining PRC2 gene expression in animals and, through this mechanism, the repression of their targets. Furthermore, in cases where multiple genes have been found to encode a single PRC2 subunit, the expression patterns of these subunits and their upstream regulation should be systematically explored. Epigenetic abnormalities are common in human cancer and play a key role in tumor progression; hence, significant efforts have focused on developing inhibitors of these PRC2 proteins to treat disease (Helin and Dhanak, 2013). The characterization of cell-type- or tissue-specific regulation of PRC2 gene expression may provide an additional mode by which the negative effects caused by PRC2 misregulation could be abrogated.

METHODS

Plant Material

All transgenic *Arabidopsis thaliana* plants and mutants are in the Col-0 background except for the VRN2$_{pro}$:VRN2:GUS line (kindly provided by Caroline Dean), which is in the L*er* background, as is the FIEpro:FIE:GFP line (Kinoshita et al., 2001). The *clf-28 swn-7* (SALK_139371, SALK_109121), *clf-29* (SALK_021003), *swn-7* (SALK_109121), and *fie* (SALK_042962) (Bouyer et al., 2011) mutants were kindly provided by François Roudier and Daniel Bouyer. The DOF6 β-estradiol inducible, VND7 and ARF17 transcriptional, and FIE in *fie-1* and SWN and MEA in *mea-3* translational fusions have been described elsewhere (Rueda-Romero et al., 2012; Yamaguchi et al., 2010; Rademacher et al., 2011; Yadegari et al., 2000; Wang et al., 2006). TF-inducible lines were obtained from the TRANSPLANTA collection (Coego et al., 2014).

Plants were grown under standard conditions at 24°C in a 16-h-light/8-h-dark cycle. For root analyses, plants surfaced sterilized and sown in 1% sucrose Murashige and Skoog (1% MS) medium. Seeds were stratified for 3 d at 4°C and dark and then transferred and kept vertical into a Percival growth chamber with a light intensity of ~700 mol m^{-2} s^{-1} illuminated by a daylight-white fluorescence lamp (FL40SS ENW/37; Panasonic). Selection of transgenic seedlings were performed in 1% MS medium supplemented with 50 mg L^{-1} kanamycin or 15 mg L^{-1} glufosinate ammonium, depending on the transgene.

Cloning Strategies

All oligonucleotides used in this study are described in Supplemental Data Set 4. All PCR-amplified fragments were completely sequenced after subcloning, and only the clones without PCR-induced errors were used for subsequent cloning steps. For promoter amplification, Col-0 genomic DNA was used as template. For coding region amplification, Col-0 cDNA was used as template, except for the *CLF* coding region, which was amplified from genomic DNA and thus contains introns. For the generation of the transcriptional GUS fusions, each respective PCR product was introduced into pENTR D-TOPO (Invitrogen) and subsequently recombined into the pGWB4 and pGWB5 destination vectors (Nakagawa et al., 2007) with the exception of the *CLF* promoter, which was assembled to Venus-N7 (rapidly folding YFP variant) by Hot Fusion reaction (Fu et al., 2014) into the *Bsa*I-digested pGoldenGate-Se7 (Emami et al., 2013).

For the CLF translational fusion shown in Figure 2, the *CLF* genomic region was amplified (primers CLF_TOPO_F_NO_ATG/CLF_R) and introduced into pENTR/D-Topo (Invitrogen). The gCLF_D_Topo clone was introduced into the pB7WGC2 binary vector to generate a CFP:gCLF fusion. The ECFP:gCLF sequence was then amplified (ECFP_TOPO_F/CLF_R) and introduced into pENTR/D-Topo. The -2842 DNA sequence

corresponding to the *CLF* promoter was amplified (pCLF_F/pCLF_R) and cloned into pENTR 5′TA-TOPO. A MultiSite Gateway reaction was performed using CLFpro-TA-Topo, CFP:gCLF-D-Topo, and the pK7m34GW destination vector. The CLFpro:CFP:gCLF transgene was introduced into the *clf-29* background by floral dip transformation (Clough and Bent, 1998), and a complementation assay was performed on T2 plants to validate a 3:1 segregation ratio. For the *CLF* genomic fusion shown in Supplemental Figure 7B, a genomic region of *CLF* including 2175 bp upstream from the start codon and 1010 bp downstream from the stop codon was amplified with primers D-TOPO-genomic_CLF_s2 and genomic_CLF_as2, following with primers genomic_CLF_s1 and genomic_CLF_as1, using PrimeSTAR Max DNA polymerase (Takara). The PCR product was cloned into pENTR/D-Topo (Thermo Fisher Scientific), and an error-free entry clone, pENTR-gCLF, was confirmed by sequence analyses. An mGFP sequence with a GGGS-linker at its N terminus was inserted into pENTR-gCLF at the site before the stop codon of CLF in frame by the circular polymerase extension cloning method, following the amplification of pENTR-gCLF and linker-mGFP with primers CLF ter_s and CLF body-Δstop_as and primers CLF body-mGFP_s and mGFP-CLF ter_as, respectively. A recombination reaction was performed between the resulting entry clone, pENTR-gCLF-mGFP, and destination vector pGWB501 (Nakagawa et al., 2007) using LR Clonase II enzyme mix (Invitrogen). Error-free destination clone was confirmed by sequence analyses and introduced into *Agrobacterium tumefaciens* strain GV3101::pMP90 by electroporation. The transgene was introduced into the *clf-28*+/−; *swn-7*−/− background by floral dip transformation of *clf-28*-/+; *swn-7*−/− plants. A complementation assay was performed to validate the function of the fusion protein. For the other translational GFP fusions, gene promoters were also introduced into pENTR 5′TA-TOPO; gene cDNAs were introduced into pENTR D-TOPO, and the *mGFP5* reporter gene was introduced into pDONOR P2r-P3. Plasmids containing the promoter, gene, and *GFP* were introduced into pB7m34GW (Karimi et al., 2005) by a Multisite Gateway reaction (Invitrogen).

The design of the amiRNA for *MSI1* was performed following WMD3 software (Ossowski et al., 2008) and cloned into pENTR D-TOPO. Afterwards, a Multisite Gateway reaction was performed in combination with the promoter of *WOL* (kindly provided by Anthony Bishopp, University of Nottingham) and pK7m24GW (Karimi et al., 2005). The resulting plasmids were introduced into Agrobacterium strain GV3101 carrying the pSoup plasmid (Hellens et al., 2000), and Col-0 wild type in addition to MSI1$_{pro}$:MSI1:GFP were transformed using floral dip (Clough and Bent, 1998). Transformation into the MSI1$_{pro}$:MSI1:GFP background served as a control to ensure precise tissue-specific silencing of MSI1 with the designed amiRNA.

Arabidopsis Cross Sections

Five-day-old roots were embedded in 3% agarose (PELCO 21 Cavity EM Embedding Mold) and incubated overnight at 4°C in fixation buffer (2.5% glutaldehyde + 2% paraformaldehyde in 0.2 M phosphate buffer, pH 7). Dehydration was performed by incubating the sample for 2 h in serial dilutions of ethanol (20, 40, 60, 80, 90, and 95%). The sample was plastic embedded by performing the following steps: 2 h incubation in 1:1 ethanol: acetone, 2 h incubation in 100% acetone, 12 h incubation in 7:1 acetone: Spurr's resin, 12 h incubation in 3:1 acetone:Spurr's resin, 12 h incubation in 100% Spurr's resin, and 12 h incubation in Spurr's resin. The resin was polymerized at 70°C for 12 h. Blocks were trimmed, and 1.5-μm cross sections were produced with a Leica 2050 SuperCut microtome. Toluidine blue staining (0.1% of Toluidine blue in 0.1 M phosphate buffer, pH 6.8) was performed before microscopy analysis.

The mPS-PI staining method (Truernit et al., 2008) combined with confocal microscopy was used for the acquisition of high-resolution root longitudinal and Z-stack images of ARF17ox plants under mock and β-estradiol treatments.

Gene Regulatory Network Mapping

Promoter sequences for PRC2 genes are described in Supplemental Data Set 2. Yeast one-hybrid screening was performed as described (Gaudinier et al., 2011). Correlations between predicted transcription factors and targets were determined using root spatial temporal microarray data sets found in Brady et al. (2007). For simplicity, the data were transformed to contain the $\log_2$ mean expression value for each sample. A Pearson correlation was calculated for each network-predicted TF-promoter interaction set. Interactions with a Benjamini-Hochberg false discovery rate corrected P value ≤0.05 were considered significant. P values for the Benjamini-Hochberg correction were determined from correlations of all possible TF-promoter combinations of each node within the network.

Validation and the direction of the yeast one-hybrid interactions were characterized in vivo by performing transactivation assays in *Nicotiana benthamiana* leaves and gene expression analyses in Arabidopsis estradiol-inducible transcription factor lines. For transactivation assays, transcription factors in PYL436 (effector) (Ma et al., 2013; collection kindly provided by Dinesh Kumar, UC Davis), promoter:GUS (reporter), 35S$_{pro}$:LUCIFERASE (internal control), and p19 (RNA silencing inhibitor) constructs were transformed into Agrobacterium (strain GV3101) and used as described (Taylor-Teeples et al., 2015). In Arabidopsis, 12- and 24-h treatments in liquid 1% MS supplemented with 10 μM β-estradiol (from a 10 mM stock in 100% DMSO) was used to induce the expression of each transcription factor in 5-d-old seedlings. Quantification of transcription factor and PRC2 gene expression was performed by RT-qPCR. We calculated the mean from three independent experiments (biological replicates) and from the average of three technical replicates per biological replicate. Each biological replicate captures expression from ~200 roots of each respective genotype. In each case, the ΔΔCt was calculated relative to a Ubiquitin10 control (At4g05320). In all cases, significance was tested using a *t* test (*P < 0.05, **P < 0.01, and ***P < 0.001).

We used Cytoscape software (Shannon et al., 2003) for data visualization and GO analysis of the network.

Whole-Mount H3K27me3 Immunohybridization of Arabidopsis Roots

The protocol was adapted from She et al. (2014). Roots of 5-d-old plants were fixed in fixation buffer (1× PBS, 2 mM EGTA, 1% formaldehyde, 10% DMSO, and 1% Tween 20) for 30 min at room temperature and then mounted in 5% acrylamide on a microscope slide. Samples were fixed by incubating them for 5 min in 100% ethanol, 5 min in 100% methanol, 30 min in methanol: xylene (1:1), 5 min in methanol, 5 min in ethanol, and 15 min in methanol:PBS (1.37 M NaCl, 27 mM KCl, 100 mM Na$_2$HPO$_4$, and 18 mM KH$_2$PO$_4$, pH 7.4) + 0.1% Tween 20 (1:1) + 2.5% formaldehyde. The samples were then rinsed with PBS + 0.1% Tween 20 and cell walls were digested for 2 h at 37°C with cell wall digestion solution (0.5% cellulase, 1% driselase, and 0.5% pectolyase in PBS). After rinsing with PBS + 0.1% Tween 20, the samples were permeabilized in PBS + 2% Tween 20 for 2 h. Immunodetection was performed using antibodies against H3K27me3 (Millipore 07-449), H3K4me3 (Millipore 07-473), and H3 (ab1791) as a control at 0.01 μg/μL final concentration each, for 14 h. Samples were washed for 4 h with PBS + 0.1% Tween 20 and incubated for 12 h with goat anti-rabbit (Alexa fluor 488 conjugate) secondary antibody (Life Technologies A-11034A). Samples were washed with 1× PBS + 0.1% Tween 20 for 1 h, and nuclei were counterstained with propidium iodide at a concentration of 5 μg/mL for 15 min, rinsed with PBS + 0.1% Tween 20, and mounted in Prolong Gold (Invitrogen) + 5 μg/mL propidium iodide. Samples were imaged using a Zeiss 700 (Genome Center, University of California, Davis). Simultaneous detection of Alexa fluor 488 and propidium iodide signal was performed using the same settings among the different samples/mutants (10 to 15 roots were studied for each mutant line).

Fluorescence-Activated Cell Sorting

Arabidopsis WOL$_{pro}$:GFP root protoplast were prepared as described (Brady et al., 2007). The MoFlo cell sorter's electronic configuration was modified to identify intact protoplasts above electronic and sample buffer "noise" levels by choosing a side scatter electronic threshold and by applying logarithmic scaling to the forward angle and side angle 488-nm laser light scatter signals. To collect the GFP-positive protoplasts, the green fluorescence of the GFP (530/50 detection filter) was separated from the red fluorescence (emission 670/30) of chlorophyll (Supplemental Figure 5). Protoplast chromatin was cross-linked with 0.1% formaldehyde for 5 min and the reaction was stopped by adding glycine (0.125 M final concentration).

ChIP Assay

The ChIP assay performed in this study is a modification of the protocol described by Bouyer et al. (2011). We used four independent biological replicates (100,000 GFP positive protoplast each) and two antibodies: H3K27me3 (Millipore 07-449) and H3K4me3 (Millipore 07-473). DNA recovered after ChIP and the input chromatin were both amplified using a SeqPlex Enhanced DNA amplification kit (SEQXE; Sigma-Aldrich) following the manufacturer's instructions. Amplified DNA was used to synthesize a barcoded Illumina-compatible library (Kumar et al., 2012). Libraries were pooled and sequenced on the HiSeq 2000 in 50SR mode.

ChIP-Seq Data Analysis

Reads were filtered by length and quality and aligned to the Arabidopsis (TAIR10) genome using Bowtie (Langmead et al., 2009) and the parameters "-v2 -m1–best–strata –S". SICER software was used to determine the differentially methylated islands using a 200-bp window size, 200-bp gap size, and a false discovery rate of 0.005. The genomic regions containing the histone modification were determined using windowbed software (Quinlan and Hall, 2010) and −1000 bp upstream and downstream of the gene body for H3K27me3 and 200 bp upstream and 200 bp downstream for H3K4me3. Genes that overlap in at least three of the four biological replicates were considered as high confidence genes for the downstream analyses.

Root cell-type-specific expression of the H3K27me3 and H3K4me3 affected genes was obtained from Brady et al. (2007). Raw expression values were $\log_2$ transformed and graphed with R software and the ggplot2 package.

GUS Expression Analysis in Arabidopsis

Plant tissue was fixed in 90% acetone for 30 min and washed twice with water before GUS staining. Roots were submerged in the GUS staining solution (50 mM phosphate buffer, 0.2% Triton TX-100, 1.5 mM potassium ferrocyanide, 1.5 mM potassium ferricyanide, and 2 mM X-Gluc (5-bromo-4-chloro-3-indolyl β-D-glucuronide cyclohexamine salt dissolved in DMSO; Gold Biotechnology G1281C1), infiltrated under vacuum for 5 min, and incubated at 37°C in the dark for 18 h. Roots were then washed with increasing concentrations of diluted ethanol (20, 35, 50, and 70%) and then mounted with Hoyer's solution on microscope slides. The activity of the GUS reporter gene was observed under a Zeiss Axioscope 2 fluorescence microscope.

In Situ Hybridization

The ARF17 and CLF coding region was PCR amplified using Col-0 cDNA and the set of primers ARF17_cDNA_F/ARF17_cDNA_ R and CLF_TOPO_F_NO_ATG/CLF_R(no_STOP). PCR product was cloned into pGEMTeasy (Promega). Fluorescein-labeled sense and antisense probes were performed according to the manufacturer's indications (Fluorescein RNA labeling mix; Roche). Tissue fixation, permeabilization, probe hybridization, and detection were adapted from Bruno et al. (2011). Probe detection was performed using horseradish peroxidase-conjugated anti-FITC antibody (1:100 dilution)

(AB6656; Abcam), followed by tyramide signal amplification (TSA reagent, Alexa Fluor 488 Tyramide; Molecular Probes). Tissue was then counterstained with propidium iodide (5 μg/mL) for 5 min and rinsed in water, and the samples were mounted with antifade reagent (Prolong gold; Molecular Probes). Samples were imaged using a Zeiss 880 with Ayriscan (Department of Biosciences, Durham University). Simultaneous detection of Alexa fluor 488 and propidium iodide signal was performed using the same settings among the different samples (10 to 15 roots were studied for each mutant line).

Accession Numbers

Sequence data from this article can be found in the GenBank/EMBL libraries under accession number GSE86429. Accession numbers of major genes mentioned are as follows: CLF, At2g23380; SWN, At4g02020; DOF6, At3g45610; VND7, At1g71930; FIE, At3g20740; ARF17, At1g77850; MEA, At1g02580; MSI1, At5g58230; FIS2, At2g35670; EMF2, At5g51230; VRN2, At4g16845.

Supplemental Data

Supplemental Figure 1. Transcriptional profile of PRC2 genes in the Arabidopsis root.

Supplemental Figure 2. DOF6 OX root phenotype, DOF6 and CLF root expression, and CLF protein abundance in the *clf28 swn7* background.

Supplemental Figure 3. ARF17ox ectopic cell proliferation data, CLFpro:CFP:CLF complementation assay, and ARF17 RNA in situ sense control.

Supplemental Figure 4. Whole-mount immunostaining of H3K27me3 and H3K4me3 deposition in Arabidopsis PRC2 mutant roots.

Supplemental Figure 5. Root cellular resolution phenotypes of different PRC2 mutants.

Supplemental Figure 6. Whole-mount immunostaining of H3K27me3 in the pWOL:amiRNA_MSI1 Arabidopsis line.

Supplemental Figure 7. Vascular-specific analysis of H3K27me3 deposition for the fluorescence-activated cell sorting of the stele (WOLpro:GFP).

Supplemental Figure 8. Transcriptional profiles of the transcription factors upstream of PRC2 genes.

Supplemental Data Set 1. H3K27me3 and H3K4me3 genes in the vascular cylinder and whole root and associated GO categories.

Supplemental Data Set 2. Protein-DNA interaction network and promoter sequences for the different PRC2 genes studied.

Supplemental Data Set 3. PRC2 network validation.

Supplemental Data Set 4. Primer sequences.

AUTHOR CONTRIBUTIONS

M.d.L. designed and performed experiments, analyzed data, discussed results, and wrote the article. L.P. performed experiments and analyzed data. G.T. performed computational analyses. A.G. performed experiments. A.K.M., H.H., D.K., and M.R. performed experiments. K.S. designed experiments with H.H. and analyzed data. F.R. designed experiments with A.K.M. and contributed to writing the manuscript. S.M.B. designed experiments, discussed results, and wrote the article.

REFERENCES

Aichinger, E., Villar, C.B.R., Di Mambro, R., Sabatini, S., and Köhler, C. (2011). The CHD3 chromatin remodeler PICKLE and polycomb group proteins antagonistically regulate meristem activity in the Arabidopsis root. Plant Cell **23:** 1047–1060.

Aldiri, I., and Vetter, M.L. (2009). Characterization of the expression pattern of the PRC2 core subunit Suz12 during embryonic development of *Xenopus laevis*. Dev. Dyn. **238:** 3185–3192.

Bemer, M., and Grossniklaus, U. (2012). Dynamic regulation of Polycomb group activity during plant development. Curr. Opin. Plant Biol. **15:** 523–529.

Benfey, P.N., and Scheres, B. (2000). Root development. Curr. Biol. **10:** R813–R815.

Birnbaum, K., Shasha, D.E., Wang, J.Y., Jung, J.W., Lambert, G.M., Galbraith, D.W., and Benfey, P.N. (2003). A gene expression map of the Arabidopsis root. Science **302:** 1956–1960.

Bouyer, D., Roudier, F., Heese, M., Andersen, E.D., Gey, D., Nowack, M.K., Goodrich, J., Renou, J.-P., Grini, P.E., Colot, V., and Schnittger, A. (2011). Polycomb repressive complex 2 controls the embryo-to-seedling phase transition. PLoS Genet. **7:** e1002014.

Bracken, A.P., Pasini, D., Capra, M., Prosperini, E., Colli, E., and Helin, K. (2003). EZH2 is downstream of the pRB-E2F pathway, essential for proliferation and amplified in cancer. EMBO J. **22:** 5323–5335.

Brady, S.M., et al. (2011). A stele-enriched gene regulatory network in the Arabidopsis root. Mol. Syst. Biol. **7:** 459.

Brady, S.M., Orlando, D.A., Lee, J.Y., Wang, J.Y., Koch, J., Dinneny, J.R., Mace, D., Ohler, U., and Benfey, P.N. (2007). A high-resolution root spatiotemporal map reveals dominant expression patterns. Science **318:** 801–806.

Bruno, L., Muto, A., Spadafora, N.D., Iaria, D., Chiappetta, A., Van Lijsebettens, M., and Bitonti, M.B. (2011). Multi-probe in situ hybridization to whole mount Arabidopsis seedlings. Int. J. Dev. Biol. **55:** 197–203.

Chanvivattana, Y., Bishopp, A., Schubert, D., Stock, C., Moon, Y.-H., Sung, Z.R., and Goodrich, J. (2004). Interaction of Polycomb-group proteins controlling flowering in Arabidopsis. Development **131:** 5263–5276.

Ciferri, C., Lander, G.C., Maiolica, A., Herzog, F., Aebersold, R., and Nogales, E. (2012). Molecular architecture of human polycomb repressive complex 2. eLife **1:** e00005.

Clough, S.J., and Bent, A.F. (1998). Floral dip: a simplified method for Agrobacterium-mediated transformation of *Arabidopsis thaliana*. Plant J. **16:** 735–743.

Coego, A., Brizuela, E., Castillejo, P., Ruíz, S., Koncz, C., del Pozo, J.C., Piñeiro, M., Jarillo, J.A., Paz-Ares, J., and León, J.; TRANSPLANTA Consortium (2014). The TRANSPLANTA collection of Arabidopsis lines: a resource for functional analysis of transcription factors based on their conditional overexpression. Plant J. **77:** 944–953.

Deal, R.B., and Henikoff, S. (2010). A simple method for gene expression and chromatin profiling of individual cell types within a tissue. Dev. Cell **18:** 1030–1040.

De Lucia, F., Crevillen, P., Jones, A.M.E., Greb, T., and Dean, C. (2008). A PHD-polycomb repressive complex 2 triggers the epigenetic silencing of FLC during vernalization. Proc. Natl. Acad. Sci. USA **105:** 16831–16836.

Deng, W., Buzas, D.M., Ying, H., Robertson, M., Taylor, J., Peacock, W.J., Dennis, E.S., and Helliwell, C. (2013). Arabidopsis Polycomb Repressive Complex 2 binding sites contain putative GAGA factor binding motifs within coding regions of genes. BMC Genomics **14:** 593.

Derkacheva, M., Steinbach, Y., Wildhaber, T., Mozgová, I., Mahrez, W., Nanni, P., Bischof, S., Gruissem, W., and Hennig, L. (2013). Arabidopsis MSI1 connects LHP1 to PRC2 complexes. EMBO J. **32:** 2073–2085.

De Rybel, B., et al. (2014). Plant development. Integration of growth and patterning during vascular tissue formation in Arabidopsis. Science **345:** 1255215.

Dolan, L., Janmaat, K., Willemsen, V., Linstead, P., Poethig, S., Roberts, K., and Scheres, B. (1993). Cellular organisation of the *Arabidopsis thaliana* root. Development **119:** 71–84.

Du, Z., Zhou, X., Ling, Y., Zhang, Z., and Su, Z. (2010). agriGO: a GO analysis toolkit for the agricultural community. Nucleic Acids Res. **38:** W64–W70.

Emami, S., Yee, M.-C., and Dinneny, J.R. (2013). A robust family of Golden Gate *Agrobacterium* vectors for plant synthetic biology. Front. Plant Sci. **4:** 339.

Etchells, J.P., Provost, C.M., Mishra, L., and Turner, S.R. (2013). WOX4 and WOX14 act downstream of the PXY receptor kinase to regulate plant vascular proliferation independently of any role in vascular organisation. Development **140:** 2224–2234.

Etchells, J.P., and Turner, S.R. (2010). Orientation of vascular cell divisions in Arabidopsis. Plant Signal. Behav. **5:** 730–732.

Fasano, C.A., Dimos, J.T., Ivanova, N.B., Lowry, N., Lemischka, I.R., and Temple, S. (2007). shRNA knockdown of Bmi-1 reveals a critical role for p21-Rb pathway in NSC self-renewal during development. Cell Stem Cell **1:** 87–99.

Fisher, K., and Turner, S. (2007). PXY, a receptor-like kinase essential for maintaining polarity during plant vascular-tissue development. Curr. Biol. **17:** 1061–1066.

Fu, C., Donovan, W.P., Shikapwashya-Hasser, O., Ye, X., and Cole, R.H. (2014). Hot Fusion: an efficient method to clone multiple DNA fragments as well as inverted repeats without ligase. PLoS One **9:** e115318.

Gaudinier, A., et al. (2011). Enhanced Y1H assays for Arabidopsis. Nat. Methods **8:** 1053–1055.

He, C., Chen, X., Huang, H., and Xu, L. (2012). Reprogramming of H3K27me3 is critical for acquisition of pluripotency from cultured Arabidopsis tissues. PLoS Genet. **8:** e1002911.

Helin, K., and Dhanak, D. (2013). Chromatin proteins and modifications as drug targets. Nature **502:** 480–488.

Hellens, R.P., Edwards, E.A., Leyland, N.R., Bean, S., and Mullineaux, P.M. (2000). pGreen: a versatile and flexible binary Ti vector for Agrobacterium-mediated plant transformation. Plant Mol. Biol. **42:** 819–832.

Hennig, L., and Derkacheva, M. (2009). Diversity of Polycomb group complexes in plants: same rules, different players? Trends Genet. **25:** 414–423.

Hennig, L., Taranto, P., Walser, M., Schönrock, N., and Gruissem, W. (2003). Arabidopsis MSI1 is required for epigenetic maintenance of reproductive development. Development **130:** 2555–2565.

Hirabayashi, Y., Suzki, N., Tsuboi, M., Endo, T.A., Toyoda, T., Shinga, J., Koseki, H., Vidal, M., and Gotoh, Y. (2009). Polycomb limits the neurogenic competence of neural precursor cells to promote astrogenic fate transition. Neuron **63:** 600–613.

Ikeuchi, M., et al. (2015). PRC2 represses dedifferentiation of mature somatic cells in Arabidopsis. Nat. Plants **1:** 15089.

Inoue, T., Higuchi, M., Hashimoto, Y., Seki, M., Kobayashi, M., Kato, T., Tabata, S., Shinozaki, K., and Kakimoto, T. (2001). Identification of CRE1 as a cytokinin receptor from Arabidopsis. Nature **409:** 1060–1063.

Jullien, P.E., Mosquna, A., Ingouff, M., Sakata, T., Ohad, N., and Berger, F. (2008). Retinoblastoma and its binding partner MSI1 control imprinting in Arabidopsis. PLoS Biol. **6:** e194.

Karimi, M., De Meyer, B., and Hilson, P. (2005). Modular cloning in plant cells. Trends Plant Sci. **10:** 103–105.

Kinoshita, T., Harada, J.J., Goldberg, R.B., and Fischer, R.L. (2001). Polycomb repression of flowering during early plant development. Proc. Natl. Acad. Sci. USA **98:** 14156–14161.

Kleer, C.G., et al. (2003). EZH2 is a marker of aggressive breast cancer and promotes neoplastic transformation of breast epithelial cells. Proc. Natl. Acad. Sci. USA **100:** 11606–11611.

Köhler, C., Hennig, L., Bouveret, R., Gheyselinck, J., Grossniklaus, U., and Gruissem, W. (2003). Arabidopsis MSI1 is a component of the MEA/FIE Polycomb group complex and required for seed development. EMBO J. **22:** 4804–4814.

Köhler, C., Page, D.R., Gagliardini, V., and Grossniklaus, U. (2005). The *Arabidopsis thaliana* MEDEA Polycomb group protein controls expression of PHERES1 by parental imprinting. Nat. Genet. **37:** 28–30.

Kubo, M., Udagawa, M., Nishikubo, N., Horiguchi, G., Yamaguchi, M., Ito, J., Mimura, T., Fukuda, H., and Demura, T. (2005). Transcription switches for protoxylem and metaxylem vessel formation. Genes Dev. **19:** 1855–1860.

Kumar, R., Ichihashi, Y., Kimura, S., Chitwood, D.H., Headland, L.R., Peng, J., Maloof, J.N., and Sinha, N.R. (2012). A high-throughput method for Illumina RNA-Seq library preparation. Front. Plant Sci. **3:** 202.

Kuzmichev, A., Margueron, R., Vaquero, A., Preissner, T.S., Scher, M., Kirmizis, A., Ouyang, X., Brockdorff, N., Abate-Shen, C., Farnham, P., and Reinberg, D. (2005). Composition and histone substrates of polycomb repressive group complexes change during cellular differentiation. Proc. Natl. Acad. Sci. USA **102:** 1859–1864.

Lafos, M., Kroll, P., Hohenstatt, M.L., Thorpe, F.L., Clarenz, O., and Schubert, D. (2011). Dynamic regulation of H3K27 trimethylation during Arabidopsis differentiation. PLoS Genet. **7:** e1002040.

Langmead, B., Trapnell, C., Pop, M., and Salzberg, S.L. (2009). Ultrafast and memory-efficient alignment of short DNA sequences to the human genome. Genome Biol. **10:** R25.

Laugesen, A., and Helin, K. (2014). Chromatin repressive complexes in stem cells, development, and cancer. Cell Stem Cell **14:** 735–751.

Ma, S., Shah, S., Bohnert, H.J., Snyder, M., and Dinesh-Kumar, S.P. (2013). Incorporating motif analysis into gene co-expression networks reveals novel modular expression pattern and new signaling pathways. PLoS Genet. **9:** e1003840.

Mähönen, A.P., Bishopp, A., Higuchi, M., Nieminen, K.M., Kinoshita, K., Törmäkangas, K., Ikeda, Y., Oka, A., Kakimoto, T., and Helariutta, Y. (2006). Cytokinin signaling and its inhibitor AHP6 regulate cell fate during vascular development. Science **311:** 94–98.

Mähönen, A.P., Bonke, M., Kauppinen, L., Riikonen, M., Benfey, P.N., and Helariutta, Y. (2000). A novel two-component hybrid molecule regulates vascular morphogenesis of the Arabidopsis root. Genes Dev. **14:** 2938–2943.

Mallory, A.C., Bartel, D.P., and Bartel, B. (2005). MicroRNA-directed regulation of Arabidopsis AUXIN RESPONSE FACTOR17 is essential for proper development and modulates expression of early auxin response genes. Plant Cell **17:** 1360–1375.

Margueron, R., and Reinberg, D. (2011). The Polycomb complex PRC2 and its mark in life. Nature **469:** 343–349.

Margueron, R., Li, G., Sarma, K., Blais, A., Zavadil, J., Woodcock, C.L., Dynlacht, B.D., and Reinberg, D. (2008). Ezh1 and Ezh2 maintain repressive chromatin through different mechanisms. Mol. Cell **32:** 503–518.

Mozgová, I., and Hennig, L. (2015). The Polycomb Group Protein Regulatory Network. Annu. Rev. Plant Biol. **66:** 269–296.

Nakagawa, T., Kurose, T., Hino, T., Tanaka, K., Kawamukai, M., Niwa, Y., Toyooka, K., Matsuoka, K., Jinbo, T., and Kimura, T. (2007). Development of series of gateway binary vectors, pGWBs, for realizing efficient construction of fusion genes for plant transformation. J. Biosci. Bioeng. **104:** 34–41.

Ohno, K., McCabe, D., Czermin, B., Imhof, A., and Pirrotta, V. (2008). ESC, ESCL and their roles in Polycomb Group mechanisms. Mech. Dev. **125:** 527–541.

Okushima, Y., et al. (2005). Functional genomic analysis of the AUXIN RESPONSE FACTOR gene family members in Arabidopsis thaliana: unique and overlapping functions of ARF7 and ARF19. Plant Cell **17:** 444–463.

Ossowski, S., Schwab, R., and Weigel, D. (2008). Gene silencing in plants using artificial microRNAs and other small RNAs. Plant J. **53:** 674–690.

Pasini, D., Bracken, A.P., Hansen, J.B., Capillo, M., and Helin, K. (2007). The polycomb group protein Suz12 is required for embryonic stem cell differentiation. Mol. Cell. Biol. **27:** 3769–3779.

Quinlan, A.R., and Hall, I.M. (2010). BEDTools: a flexible suite of utilities for comparing genomic features. Bioinformatics **26:** 841–842.

Rademacher, E.H., Möller, B., Lokerse, A.S., Llavata-Peris, C.I., van den Berg, W., and Weijers, D. (2011). A cellular expression map of the Arabidopsis AUXIN RESPONSE FACTOR gene family. Plant J. **68:** 597–606.

Roudier, F., et al. (2011). Integrative epigenomic mapping defines four main chromatin states in Arabidopsis. EMBO J. **30:** 1928–1938.

Rueda-Romero, P., Barrero-Sicilia, C., Gómez-Cadenas, A., Carbonero, P., and Oñate-Sánchez, L. (2012). *Arabidopsis thaliana* DOF6 negatively affects germination in non-after-ripened seeds and interacts with TCP14. J. Exp. Bot. **63:** 1937–1949.

Scheres, B. (2007). Stem-cell niches: nursery rhymes across kingdoms. Nat. Rev. Mol. Cell Biol. **8:** 345–354.

Shannon, P., Markiel, A., Ozier, O., Baliga, N.S., Wang, J.T., Ramage, D., Amin, N., Schwikowski, B., and Ideker, T. (2003). Cytoscape: a software environment for integrated models of biomolecular interaction networks. Genome Res. **13:** 2498–2504.

She, W., Grimanelli, D., and Baroux, C. (2014). An efficient method for quantitative, single-cell analysis of chromatin modification and nuclear architecture in whole-mount ovules in Arabidopsis. J. Vis. Exp. **19:** e51530.

Sher, F., Rössler, R., Brouwer, N., Balasubramaniyan, V., Boddeke, E., and Copray, S. (2008). Differentiation of neural stem cells into oligodendrocytes: involvement of the polycomb group protein Ezh2. Stem Cells **26:** 2875–2883.

Sieburth, L.E., and Meyerowitz, E.M. (1997). Molecular dissection of the AGAMOUS control region shows that cis elements for spatial regulation are located intragenically. Plant Cell **9:** 355–365.

Stojic, L., et al. (2011). Chromatin regulated interchange between polycomb repressive complex 2 (PRC2)-Ezh2 and PRC2-Ezh1 complexes controls myogenin activation in skeletal muscle cells. Epigenetics Chromatin **4:** 16.

Takawa, M., et al. (2011). Validation of the histone methyltransferase EZH2 as a therapeutic target for various types of human cancer and as a prognostic marker. Cancer Sci. **102:** 1298–1305.

Taylor-Teeples, M., et al. (2015). An Arabidopsis gene regulatory network for secondary cell wall synthesis. Nature **517:** 571–575.

Terpstra, I., and Heidstra, R. (2009). Stem cells: The root of all cells. Semin. Cell Dev. Biol. **20:** 1089–1096.

Truernit, E., Bauby, H., Dubreucq, B., Grandjean, O., Runions, J., Barthélémy, J., and Palauqui, J.C. (2008). High-resolution whole-mount imaging of three-dimensional tissue organization and gene expression enables the study of phloem development and structure in Arabidopsis. Plant Cell **20:** 1494–1503.

Turck, F., Roudier, F., Farrona, S., Martin-Magniette, M.-L., Guillaume, E., Buisine, N., Gagnot, S., Martienssen, R.A., Coupland, G., and Colot, V. (2007). Arabidopsis TFL2/LHP1 specifically associates with genes marked by trimethylation of histone H3 lysine 27. PLoS Genet. **3:** e86.

Varambally, S., Dhanasekaran, S.M., Zhou, M., Barrette, T.R., Kumar-Sinha, C., Sanda, M.G., Ghosh, D., Pienta, K.J., Sewalt, R.G.A.B., Otte, A.P., Rubin, M.A., and Chinnaiyan, A.M. (2002). The polycomb group protein EZH2 is involved in progression of prostate cancer. Nature **419:** 624–629.

Wagener, N., Macher-Goeppinger, S., Pritsch, M., Hüsing, J., Hoppe-Seyler, K., Schirmacher, P., Pfitzenmaier, J., Haferkamp, A., Hoppe-Seyler, F., and Hohenfellner, M. (2010). Enhancer of zeste homolog 2 (EZH2) expression is an independent prognostic factor in renal cell carcinoma. BMC Cancer **10:** 524.

Wang, D., Tyson, M.D., Jackson, S.S., and Yadegari, R. (2006). Partially redundant functions of two SET-domain polycomb-group proteins in controlling initiation of seed development in Arabidopsis. Proc. Natl. Acad. Sci. USA **103:** 13244–13249.

Yadegari, R., Kinoshita, T., Lotan, O., Cohen, G., Katz, A., Choi, Y., Katz, A., Nakashima, K., Harada, J.J., Goldberg, R.B., Fischer, R.L., and Ohad, N. (2000). Mutations in the FIE and MEA genes that encode interacting polycomb proteins cause parent-of-origin effects on seed development by distinct mechanisms. Plant Cell **12:** 2367–2382.

Yamaguchi, M., Ohtani, M., Mitsuda, N., Kubo, M., Ohme-Takagi, M., Fukuda, H., and Demura, T. (2010). VND-INTERACTING2, a NAC domain transcription factor, negatively regulates xylem vessel formation in Arabidopsis. Plant Cell **22:** 1249–1263.

Zhang, X., Clarenz, O., Cokus, S., Bernatavichute, Y.V., Pellegrini, M., Goodrich, J., and Jacobsen, S.E. (2007a). Whole-genome analysis of histone H3 lysine 27 trimethylation in Arabidopsis. PLoS Biol. **5:** e129.

Zhang, X., Germann, S., Blus, B.J., Khorasanizadeh, S., Gaudin, V., and Jacobsen, S.E. (2007b). The Arabidopsis LHP1 protein colocalizes with histone H3 Lys27 trimethylation. Nat. Struct. Mol. Biol. **14:** 869–871.

Transcriptional Regulation of Arabidopsis Polycomb Repressive Complex 2 Coordinates Cell-Type Proliferation and Differentiation

Miguel de Lucas, Li Pu, Gina Turco, Allison Gaudinier, Ana Karina Morao, Hirofumi Harashima, Dahae Kim, Mily Ron, Keiko Sugimoto, Francois Roudier and Siobhan M. Brady

This information is current as of December 2, 2016

Supplemental Data	**http://www.plantcell.org/content/suppl/2016/09/20/tpc.15.00744.DC1.html**
References	This article cites 82 articles, 32 of which can be accessed free at: http://www.plantcell.org/content/28/10/2616.full.html#ref-list-1
Permissions	https://www.copyright.com/ccc/openurl.do?sid=pd_hw1532298X&issn=1532298X&WT.mc_id=pd_hw1532298X
eTOCs	Sign up for eTOCs at: http://www.plantcell.org/cgi/alerts/ctmain
CiteTrack Alerts	Sign up for CiteTrack Alerts at: http://www.plantcell.org/cgi/alerts/ctmain
Subscription Information	Subscription Information for *The Plant Cell* and *Plant Physiology* is available at: http://www.aspb.org/publications/subscriptions.cfm